Ann. For. Sci. 61 (2004) 251–262
© INRA, EDP Sciences, 2004
DOI: 10.1051/forest:2004018

Original article

Relationships between the intra-ring wood density assessed by X-ray densitometry and optical anatomical measurements in conifers. Consequences for the cell wall apparent density determination

Valérie DECOUX[a], Éliane VARCIN[b], Jean-Michel LEBAN[b]*

[a] Université Libre de Bruxelles, 50 av. FD Roosevelt, SAAS-CP165/55, 1050 Brussels, Belgium
[b] INRA Champenoux, Équipe Qualité des Bois, France

(Received 25 September 2002; accepted 21 May 2003)

Abstract – The objective of this work is to compare anatomical measurements to wood density variations within annual rings of three major softwood species, Norway spruce, Scots Pine and Silver Fir. The six selected annual rings were sampled within a database of thousand microdensitometric profiles measured on wood samples collected in Finland and France. Each of the six studied annual rings represents one average profile of wood density for a given age class and age ring width. The dimensions of the tracheids are performed in the radial-tangential plane by using two different planimetric methods. The wood density profile within each ring is calculated simply by the mean of the tracheid dimensions and by using a constant value for the cell wall density. We have verified that the knowledge of the (i) tracheid geometry and (ii) the usually admitted value of the cell wall density allows us to calculate intra ring wood density profiles which are similar to the X-rays wood density profiles in terms of variations but very different in average. Thus it appears necessary to calibrate by using an apparent cell wall density varying inside the rings and being far weaker than the effective cell wall density of 1460 kg/m³ as it is usually admitted in the literature.

wood density / wood anatomy / *Picea abies* / *Pinus silvestris* / *Abies alba*

Résumé – Variations intra-cerne de densité du bois et mesures optiques des caractéristiques anatomiques de résineux. Conséquences pour la détermination de la densité apparente de paroi. L'objectif de ce travail est comparer des mesures anatomiques à des mesures de variations de densité du bois à l'intérieur de cernes annuels pour trois essences résineuses importantes, l'épicéa commun, le sapin pectiné et le pin sylvestre. Les cernes sélectionnés sont choisis dans un échantillon de plusieurs milliers de cernes prélevés dans des arbres en France et en Finlande. Chaque cerne étudié représente pour une essence le profil moyen de densité d'une classe d'âge compté depuis la moelle et d'une classe de largeur de cerne. Les caractéristiques géométriques des trachéides sont mesurées par deux méthodes planimétriques différentes dans le plan radial-tangentiel. Le profil de densité du bois est calculé simplement à partir des dimensions des trachéides et de la densité de la matière ligneuse. Pour que le profil calculé de densité du bois corresponde au profil obtenu par microdensitométrie nous avons montré qu'il est nécessaire faire varier le facteur de calibration, appelé densité apparente de la paroi cellulaire, à l'intérieur des cernes avec des valeurs bien plus faibles que 1460 kg/m³, la valeur habituellement utilisée dans la littérature.

densité du bois / anatomie / *Picea abies* / *Pinus silvestris* / *Abies alba*

1. INTRODUCTION

Basically all physical properties of wood are determined by factors inherent in its structural organisation. These can be summarised as: (i) the amount or proportion of cell wall substance present in a given piece of wood and (ii) the spatial arrangement of the wall substance. Wood density is a measurement of the quantity of material contained in a certain volume but it gives no information on its spatial distribution.

As wood density provides a good but limited explanation of the wood properties, we believe that consideration of the anatomical characteristics could allow a better understanding of this material behaviour. Because the ring anatomy represents the expression of the tree genotype at a given height and cambial age and under the annual growth conditions (precipitation, temperature, soil…), it appears to be the link between the tree physiology and the wood quality.

At present, the main approach of the anatomy – wood density relationship consists of the estimation of a calibration factor called the cell wall apparent density [19, 29, 33, 41, 43, 47] based on the measurements of (i) the density of a wood sample, a wood block for gravimetry or a 2 mm thick section for X-ray

* Corresponding author: leban@nancy.inra.fr

Table I. Breakdown of the studied rings.

Species	Age of the ring (years)	Mean bulk density (kg/m^3)	Ring width (μm)	Year
Finland spruce (FinS)	36	471	2680	1938
France spruce (FraS)	35	482	2850	1956
France fir (FraF)	49	509	2760	1985
France pine (FraP)	35	527	2690	1977
North Finland pine (NFinP)	52	526	1280	1916
South Finland pine (SFinP)	54	597	2070	1954

and (ii) the cell wall proportion on its area or on a section withdrawn from it. The apparent density of the cell wall is then obtained from the wood density divided by the cell wall proportion by making the following assumptions.

The cell wall proportion is constant within each sample thickness, in other words the longitudinal tracheids and their walls are uniformly wide throughout their length. This appears reasonable as only the tracheid pits are sharp and as the tracheids are at least a few mm long.

The tracheids occupy the whole wood volume. Indeed in coniferous wood the tracheids represent more than 93 % of the total number of cells [3].

This wood density/cell wall proportion ratio should be a measure of the wood matter density (cell walls, middle lamella, walls of ray cells and canals), which is considered as cell wall density [29, 32, 43], and is sometimes called apparent density of the solid substance [47], specific gravity of the cell wall [30, 33] or packing density [18, 41].

In the literature the relationships between wood density and tracheid dimensions are difficult to compare since different variables were measured, with different techniques and on different species.

The relative importance of different tracheid dimensions on wood density can be assessed by multiple regression analysis using the criterion of adjusted R^2 [14, 21] but without taking possible serial correlation into account neither the non stationary character of the measurements all along a ring and with only a limited number of available anatomical characteristics.

In a different way, Wimmer [46] has proposed a numeric wood density model based on a rectangular and uniform tracheid shape in cross section whose differentiation allows an evaluation of how individual anatomical parameters mathematically change wood density.

The multiple linear regressions approach [14] shows that (i) the earlywood lumen diameters (radial and tangential) and (ii) the latewood proportion have both the strongest relationships with wood density. The tracheid dimensions are less good predictors for wood density at age 3–4 than at age 21–26.

For Lindström [21], wood density is found dependent on latewood percentage and the inverted value of the earlywood radial tracheid diameter ($R^2 = 0.80$). Wimmer [46] confirms the latewood percentage being a good predictor for wood density.

This study intends to compare the evolution of the intra ring density and of anatomical characteristics measured on the transverse plane all along the ring in order to obtain an anatomical interpretation of the wood density microvariations measured by X-ray. At the same time, it will be possible to compare two optical methods of measurement of the anatomical characteristics: manual (planimetry) and automated (image analysis).

The manual method implies (i) to count the total number of tracheids and (ii) to measure the cell wall thickness. Based on these figures, with the support of one simple geometric model and by the mean of the expected value for the cell wall density, it is possible to calculate the wood density variations. Such approach permits to rely simply the wood anatomy to the wood density. Two simple geometric models for the tracheids are tested in order to determine their sensitivity to the wood density calculation.

As image analysis is the most used tool for wood anatomy, we have compared the planimetric method to the image analysis method. This method involves several processes such as thresholding that can affect the cell wall proportion measurement.

Our objective is to examine for three softwood species, how the intra ring wood density can be exactly predicted by the knowledge of (i) the tracheid geometry, actual or simulated, and of (ii) the packing density of the cell wall.

2. MATERIALS AND METHODS

2.1. Samples selection

From a previous work done by the Wood Quality Team from INRA-Champenoux Centre, the microdensitometric data and the mounted microtomic sections (12 μm thick, stained with safranin) of three conifers species (*Picea abies, Pinus silvestris* and *Abies alba*) of different origins (North East France, North and South Finland) were available. The microdensitometric data were classified in age classes of 30 years and ring widths of 1 mm. Only the classes containing data for more than 50 rings and at least 5 trees were kept. For each of these classes, a mean microdensitometric profile was calculated and within our data base we have selected the ring, whose actual densitometric profile was the closest to the calculated mean profile.

Table I presents a breakdown of the studied samples.

2.2. Microdensity determinations

The densities of the six selected rings were obtained from X-ray densitometry (Joyce Loebl) of 2 mm thick sections, air dried at 12% moisture content [26, 27]. This method allows to measure density microvariations [20, 22] as the radial step of measurement may be as

Table II. X-ray densitometric values (kg/m^3) for each part of the six rings.

	1	2	3	4	5	6	7	8	9	10	11	12	13	14	15	16	17	18	19	20
FinS	363	285	299	307	319	317	316	328	340	361	397	433	455	498	554	642	713	765	864	867
FraS	351	286	289	288	300	306	318	338	364	396	420	442	456	479	516	592	685	827	962	1027
FraF	330	287	286	303	314	327	337	351	382	420	453	505	552	620	700	716	783	814	842	861
FraP	417	325	309	319	324	324	312	307	317	353	426	509	583	569	709	824	882	925	939	862
NFinP	433	371	352	361	362	354	366	376	375	378	396	425	479	530	628	746	826	921	959	875
SFinP	508	374	355	346	348	360	383	398	406	427	453	530	706	817	845	859	975	997	998	862

small as 25 µm [23, 24]. The investigated width is 1000 µm in the tangential direction.

The microdensitometric data of the six rings are presented in Table II. The rings were divided in 20 equal parts in the radial direction, a mean being calculated for each one.

2.3. Planimetric method

The six sections were photographed with an enlargement of 45. A window was disposed on each ring of a radial size equal to the ring width. The tangential width of the window depended on the width of the section and straightness of the ring limits. The selected widths were 3000 µm for Finland spruce, France spruce and France fir; 1500 µm for France pine and South Finland pine and 1000 µm for North Finland pine. When rays or canals were present, the measured area was limited to the area occupied by tracheids only.

Each ring was then divided in 20 equal parts in the radial direction.

Anatomical measurements were made by human eye with a micrometric scale integrated into a magnifying glass. The tracheids only were taken into account.

For the six rings we obtained the number of cells per length unit by counting the total number of tracheids in both radial and tangential directions. The cell wall thickness was measured for only 50 tracheids randomly selected in each of the 20 parts of each ring, for both radial and tangential directions. The total number of tracheids counted in the radial direction vary among each divided part of the rings by a factor 2. For instance this number vary from 64 up to 117 tracheids for a narrow ring (North Finland pine) and from 131 up to 240 for a wider ring (South Finland pine).

From these measurements (i) the mean tracheid sizes in the radial and tangential directions and (ii) the mean cell wall thickness were obtained for each ring.

Two simple geometric models were then used and tested in order to display these results in terms of intra ring wood density variation. The tracheids are assumed to be rectangle or hexagonal shaped in the transverse plane (Fig. 1). The second model was considered because the rectangular model does not fit well the visual pattern of the observed softwoods tracheids.

2.3.1. Rectangular model

R = mean radial size of the cell = (ring width/20) / number of cells on a radial length of (ring width/20); T = mean tangential size of the cell = width of the window of measurement / number of cells on the tangential width of the window of measurement; x = mean cell wall width, with: S = mean cell area; s' = mean lumen area; s = mean cell wall area = S – s'.

$S = R \cdot T$,

$s' = (R - 2x) \cdot (T - 2x)$.

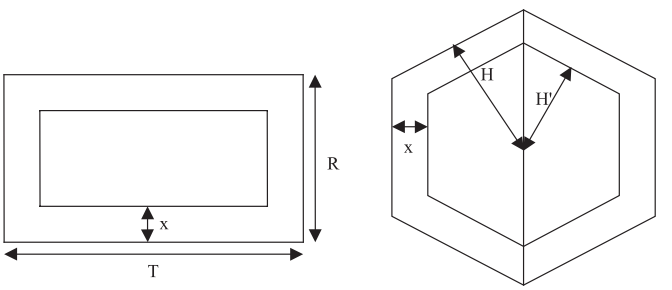

Figure 1. Rectangular (left) and hexagonal (right) cell and lumen models.

Let $X = 2 \cdot x$ = width of the double cell wall:

$s = R \cdot T - [(R - X) \cdot (T - X)]$,

$s = X \cdot (T + R) - X^2$,

s / S = cell wall proportion.

If drx = the wood density measured by x ray: apparent density of the cell wall = drx / cell wall proportion = drx · S/s

$= drx \cdot R \cdot T / [X \cdot (T + R) - X^2]$

$= drx \cdot R \cdot T / [X \cdot (T + R - X)]$.

2.3.2. Hexagonal model

S_T = area of measurement = width of the window of measurement (ring width/20); S = mean cell area = S_T / number of cells in the window of measurement; x = mean cell wall width, with: s' = mean lumen area; s = mean cell wall area = S – s'; H = height of the hexagon; H' = H – x.

As the angle between an axis passing by a corner of a hexagon and the adjacent median is of 30°: $S = 6\ H \cdot (H \cdot \tan 30°)$, as $\tan 30° = \sqrt{3}/3$, thus $S = 2 \cdot \sqrt{3} \cdot H^2$.

As well: $s' = 2 \cdot \sqrt{3} \cdot H'^2$; $s / S = (S - s') / S = 2 \cdot \sqrt{3} \cdot (H^2 - H'^2) / (2 \cdot \sqrt{3} \cdot H^2) = (H^2 - H'^2) / H^2$.

And again, if drx = the wood density measured by x ray: apparent density of the cell wall = drx / cell wall proportion = $drx \cdot S/s = drx \cdot H^2 / (H^2 - H'^2)$.

The use of rectangular and hexagonal models of cell shape allows the determination of the mean cell wall area, width and proportion. The cell wall apparent density is then obtained from the wood density/cell wall proportion ratio.

2.4. Image analysis method

Measurements were made on the same mounted sections as the planimetric method. Images of the rings were acquired at a magnification of 300 with a transmission microscope and by the use of Analysis©. At this magnification, the resolution of the images is 0.76 µm/pixel.

Table III. Planimetric and image analysis measurements on Finland spruce. Length of the window of measurement = ring width = 2680 µm; width of the window of measurement for the planimetry = 3000 µm; width of the window of measurement for image analysis = 1000 µm; Rect. = rectangular model – Hexag. = hexagonal model – Masked = masked images.

Finland spruce (FinS)													
		Planimetric measurements								Image analysis			
Parts of the ring	X-ray (kg/m^3)	Cell wall widths (µm)	Radial ϕ (µm)	Tang ϕ (µm)	Cell wall prop. Rect.	Packing density (kg/m^3) Rect.	H (µm)	Cell wall prop. Hexag.	Packing density (kg/m^3) Hexag.	Cell wall prop.	Packing density (kg/m^3)	Cell wall prop. (Masked)	Packing density (kg/m^3) (Masked)
1	363	2.9	47.4	31.0	0.284	1277	20.6	0.260	1398	0.339	1070	0.312	1163
2	285	2.8	48.2	30.8	0.278	1027	20.7	0.253	1127	0.347	821	0.329	867
3	299	2.8	44.4	30.8	0.290	1032	19.9	0.266	1123	0.351	853	0.335	893
4	307	2.9	40.6	30.8	0.303	1012	19.0	0.281	1092	0.356	863	0.342	898
5	319	2.9	41.2	30.9	0.306	1043	19.2	0.283	1126	0.360	885	0.346	922
6	317	3.0	40.1	30.1	0.315	1005	18.7	0.292	1085	0.367	863	0.351	903
7	316	3.0	39.3	29.9	0.322	982	18.4	0.298	1059	0.368	858	0.352	898
8	328	3.0	40.5	30.0	0.322	1019	18.7	0.298	1101	0.377	869	0.360	910
9	340	3.1	39.2	29.4	0.333	1021	18.2	0.308	1102	0.420	810	0.401	847
10	361	3.1	38.1	29.2	0.344	1049	17.9	0.319	1130	0.423	854	0.405	890
11	397	3.2	36.6	29.1	0.356	1116	17.5	0.331	1199	0.449	885	0.429	926
12	433	3.5	34.2	29.4	0.390	1109	17.0	0.365	1186	0.489	886	0.463	936
13	455	3.7	33.6	29.0	0.417	1090	16.8	0.391	1164	0.512	889	0.484	939
14	498	4.2	33.1	29.3	0.464	1074	16.7	0.435	1144	0.563	885	0.535	931
15	554	4.2	32.1	29.1	0.475	1166	16.4	0.446	1241	0.576	962	0.553	1002
16	642	4.9	29.5	29.7	0.555	1157	15.9	0.523	1227	0.638	1006	0.612	1050
17	713	5.3	26.0	28.9	0.624	1143	14.7	0.589	1210	0.709	1005	0.689	1035
18	765	5.7	25.3	29.2	0.669	1144	14.6	0.632	1211	0.764	1002	0.743	1029
19	864	6.4	24.0	29.6	0.737	1173	14.3	0.696	1242	0.795	1087	0.776	1114
20	867	5.8	19.1	31.1	0.756	1147	13.1	0.691	1254	0.884	980	0.873	993
Mean	471	3.8	35.6	29.9	0.427	1089	17.4	0.398	1171	0.504	917	0.485	957

The procedure of acquisition (adjustment of the microscope, its focal length and illumination) was tested and settled down to ensure its reproducibility.

The rings images have a radial size equal to the ring width and a tangential width of 1000 µm. Only the South Finland pine ring image has a width of 802 µm.

Before making any measurements on the rings images, those have to be binarized. A digital image is characterised by a grey level histogram which represents the number of pixels belonging to the 256 different grey level values (from 0 (black) to 255 (white)). The grey level histogram of a ring image is a bimodal curve consisting of a first peak of dark pixels (low grey level values) corresponding to matter (tracheids, ray cells and canals walls) and a second one of light pixels (high grey level values) corresponding to voids (lumens and pores). As matter has to be separated from voids, the rings images are binarized so that a grey level of 0 is applied on the pixels belonging to matter (for which the original grey levels are lower than the threshold value) and a grey level of 255 on the pixels belonging to the voids (for which the original grey levels are higher than the threshold value). This binarisation, meaning the choice of a threshold, is made by automatic thresholding with Labview© (National Instruments). The thresholding mode leading to the more realistic separation between material and lumen is chosen.

Each image is divided into 20 parts in the radial direction so that one threshold is applied to each of those ring parts. It is preferable to do the segmentation on parts of the image, rather than on the complete image of the ring at one time, since the grey levels of the lumens in the earlywood have a tendency to be brighter than in the latewood, in view of the differences between the architectures of early and latewood cells [5].

On each tangential pixels line of the binarized image the numbers of black pixels nbp (corresponding to matter) and white pixels nwp (corresponding to voids) are counted. The proportion of matter in area is then obtained from nbp/(nbp + nwp).

This proportion of matter was measured at first on the images of the whole rings and then on images of tracheids only (on which the rays, canals and defects were excluded).

When measuring the proportion of matter on the whole images, the walls of tracheids, rays and canals are considered. The ratio wood density / proportion of matter gives thus a measure of the apparent density of the tracheids, rays and canals walls. When only the tracheids are considered, the tracheid wall proportion is measured and the apparent density of the tracheid wall calculated.

3. RESULTS (TABS. III TO VIII)

The density of wood increases all along the period of a growth ring as a consequence of anatomical and chemical modifications. The mean variation for the six studied rings is

Table IV. Planimetric and image analysis measurements on France spruce. Length of the window of measurement = ring width = 2850 μm; width of the window of measurement for the planimetry = 3000 μm; width of the window of measurement for image analysis = 1000 μm.

France spruce (FraS)													
		Planimetric measurements								Image analysis			
Parts of the ring	X-ray (kg/m^3)	Cell wall widths (μm)	Radial ϕ (μm)	Tang ϕ (μm)	Cell wall prop. Rect.	Packing density (kg/m^3) Rect.	H (μm)	Cell wall prop. Hexag.	Packing density (kg/m^3) Hexag.	Cell wall prop.	Packing density (kg/m^3)	Cell wall prop. (Masked)	Packing density (kg/m^3) (Masked)
1	351	3.1	41.4	32.8	0.309	1136	19.8	0.287	1222	0.346	1015	0.319	1100
2	286	2.8	42.0	33.2	0.284	1005	20.0	0.264	1082	0.341	839	0.322	889
3	289	2.9	39.2	33.3	0.293	986	19.4	0.273	1057	0.352	820	0.330	875
4	288	2.9	38.7	33.7	0.295	977	19.4	0.275	1046	0.358	804	0.343	839
5	300	2.9	36.9	33.6	0.307	977	18.9	0.287	1045	0.365	822	0.349	860
6	306	3.0	35.8	33.2	0.315	971	18.5	0.295	1037	0.364	840	0.348	878
7	318	3.2	40.1	32.9	0.325	979	19.5	0.303	1050	0.374	850	0.360	884
8	338	3.5	41.0	32.1	0.352	960	19.5	0.327	1032	0.385	878	0.371	911
9	364	3.7	39.9	31.9	0.372	979	19.2	0.346	1051	0.411	885	0.395	922
10	396	3.7	36.5	31.6	0.391	1013	18.3	0.366	1083	0.435	909	0.423	937
11	420	4.2	34.1	31.3	0.448	937	17.6	0.421	998	0.448	937	0.438	960
12	442	4.1	35.6	31.6	0.427	1036	18.0	0.400	1105	0.469	943	0.458	965
13	456	4.3	36.0	31.1	0.446	1023	18.0	0.418	1091	0.470	971	0.459	993
14	479	4.3	36.0	31.5	0.446	1075	18.1	0.418	1146	0.487	983	0.478	1003
15	516	4.8	34.2	31.6	0.496	1040	17.7	0.467	1106	0.520	992	0.509	1015
16	592	5.1	30.9	31.0	0.549	1078	16.6	0.518	1142	0.578	1024	0.568	1043
17	685	5.2	27.5	30.8	0.593	1156	15.6	0.559	1225	0.647	1058	0.636	1077
18	827	5.8	26.0	30.5	0.662	1250	15.1	0.625	1324	0.731	1131	0.725	1141
19	962	6.1	22.6	31.2	0.721	1334	14.3	0.674	1428	0.803	1198	0.797	1208
20	1027	6.1	19.2	32.5	0.776	1323	13.4	0.706	1455	0.869	1181	0.865	1188
Mean	482	4.1	34.7	32.1	0.440	1062	17.8	0.411	1136	0.488	954	0.475	984

a LW (latewood) density about 3 times greater than the EW (earlywood) density, that is in the range of the 1 to 4 times variation already reported [16]. The evolution of density is also more abrupt in the LW [28].

3.1. Planimetric method

Based upon (i) the anatomical measurements and (ii) the geometric model, the intra ring density variation is readily displayed in order to compare with the measured X-ray density profile. For the six rings, when multiplying the calculated cell wall proportion with the accepted cell wall density value of 1530 kg/m³ [36], the obtained wood density profile is higher than the measured one (Fig. 2). The use of a rectangular model leads to higher cell wall proportion, thus an even higher calculated wood density than the hexagonal one due to mathematical considerations. It seems preferable to use the hexagonal model as it also fits the real tracheid shape better.

The calculated apparent densities of the cell wall vary along the six rings between 1030 and 1460 kg/m³, values quite far from 1530 kg/m³. Those densities vary from EW (mean value for the six rings of 1140 kg/m³) to LW (mean value of 1360 kg/m³). This increase of the apparent density of the cell wall shows that the cell wall proportion alone (rendering the anatomical variations) is not responsible of the entire wood density increase from EW to LW.

3.2. Image analysis method

As with planimetry, the wood density is over estimated when applying a density of 1530 kg/m³ to the measured cell wall proportion (Fig. 3). The exclusion of rays and canals smoothes the measurements as it excludes local characteristics. This is illustrated on Figure 4. On this figure we have reported the X-ray wood density measurement and the wood density profiles calculated by the mean of the cell wall proportion obtained by image analysis of the sections. The cell wall proportion is measured (i) for the whole image (tracheids and resin canals) and measured (ii) for tracheids only. For all the rings but especially the FraS sample (Fig. 5), the exclusion decreases the measured proportion of matter, especially in the earlywood.

The calculated apparent densities of (tracheids, rays and canals) walls vary between 880 in the EW and 1140 kg/m³ in the LW and the apparent densities of the tracheids walls range from 940 to 1150 kg/m³, values again quite far from 1530 kg/m³.

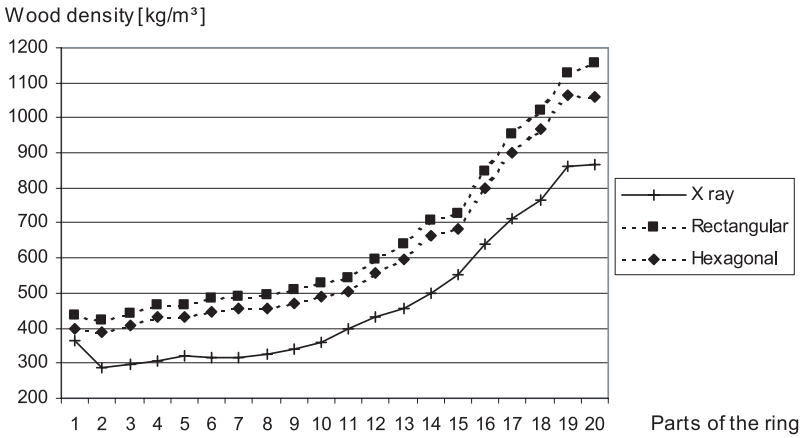

Figure 2. Finland spruce ring: Wood density measured by X-ray and calculated from the cell wall proportion (rectangular and hexagonal model) and a cell wall density of 1530 kg/m³.

Table V. Planimetric and image analysis measurements on France pine. Length of the window of measurement = ring width = 2690 µm; width of the window of measurement for the planimetry = 1500 µm; width of the window of measurement for image analysis = 1000 µm.

France fir (FraF)													
		Planimetric measurements								Image analysis			
Parts of the ring	X-ray (kg/m^3)	Cell wall widths (µm)	Radial ϕ (µm)	Tang ϕ (µm)	Cell wall prop. Rect.	Packing density (kg/m^3) Rect.	H (µm)	Cell wall prop. Hexag.	Packing density (kg/m^3) Hexag.	Cell wall prop.	Packing density (kg/m^3)	Cell wall prop. (Masked)	Packing density (kg/m^3) (Masked)
1	330	2.6	42.9	29.2	0.282	1172	19.0	0.258	1277	0.343	963	0.301	1097
2	287	2.5	43.2	29.6	0.262	1096	19.2	0.240	1194	0.322	892	0.288	995
3	286	2.5	42.7	29.9	0.266	1077	19.2	0.244	1171	0.321	892	0.291	982
4	303	2.6	42.6	29.9	0.271	1117	19.2	0.250	1214	0.332	914	0.302	1003
5	314	2.7	41.9	30.9	0.277	1133	19.3	0.256	1225	0.331	947	0.300	1045
6	327	2.8	40.9	31.2	0.291	1123	19.2	0.270	1212	0.357	917	0.329	995
7	337	3.0	41.6	30.8	0.307	1096	19.2	0.284	1185	0.362	930	0.333	1012
8	351	3.1	39.3	30.5	0.332	1058	18.6	0.308	1139	0.378	928	0.347	1011
9	382	3.2	35.9	30.4	0.350	1092	17.7	0.327	1169	0.398	959	0.366	1043
10	420	3.4	36.1	30.7	0.366	1147	17.9	0.342	1227	0.431	974	0.401	1048
11	453	3.6	34.8	30.7	0.395	1148	17.6	0.369	1226	0.465	974	0.435	1041
12	505	3.9	31.5	30.6	0.436	1157	16.7	0.410	1232	0.510	990	0.486	1039
13	552	4.2	30.5	31.2	0.475	1162	16.6	0.447	1235	0.539	1024	0.516	1071
14	620	4.6	27.6	30.5	0.532	1166	15.6	0.500	1239	0.598	1037	0.573	1081
15	700	4.7	25.8	29.0	0.574	1219	14.7	0.541	1294	0.647	1082	0.624	1122
16	716	4.8	26.5	29.4	0.574	1248	15.0	0.541	1324	0.651	1100	0.626	1143
17	783	5.1	23.7	28.9	0.633	1237	14.0	0.595	1315	0.711	1102	0.688	1138
18	814	5.3	24.0	28.4	0.648	1257	14.0	0.610	1334	0.740	1100	0.716	1137
19	842	5.3	22.6	28.6	0.667	1262	13.7	0.627	1343	0.730	1154	0.704	1196
20	861	5.1	18.3	28.7	0.712	1209	12.3	0.654	1316	0.770	1119	0.750	1148
Mean	509	3.8	33.6	30.0	0.432	1159	16.9	0.404	1244	0.497	1000	0.469	1067

Table VI. Planimetric and image analysis measurements on France pine. Length of the window of measurement = ring width = 2690 µm; width of the window of measurement for the planimetry = 1500 µm; width of the window of measurement for image analysis = 1000 µm.

France pine (FraP)													
		Planimetric measurements								Image analysis			
Parts of the ring	X-ray (kg/m^3)	Cell wall widths (µm)	Radial ϕ (µm)	Tang ϕ (µm)	Cell wall prop. Rect.	Packing density (kg/m^3) Rect.	H (µm)	Cell wall prop. Hexag.	Packing density (kg/m^3) Hexag.	Cell wall prop.	Packing density (kg/m^3)	Cell wall prop. (Masked)	Packing density (kg/m^3) (Masked)
1	417	3.4	40.9	29.7	0.354	1178	18.7	0.327	1274	0.380	1098	0.367	1137
2	325	3.3	48.0	30.0	0.324	1002	20.4	0.295	1102	0.355	915	0.345	941
3	309	3.1	47.0	29.7	0.311	995	20.1	0.283	1093	0.366	843	0.361	855
4	319	3.2	46.7	29.7	0.321	995	20.0	0.292	1092	0.354	902	0.355	898
5	324	3.2	45.3	29.9	0.323	1004	19.8	0.295	1097	0.351	923	0.350	926
6	324	3.2	44.4	29.6	0.327	991	19.5	0.299	1082	0.362	894	0.353	918
7	312	3.2	47.7	29.6	0.320	975	20.2	0.291	1073	0.330	945	0.328	951
8	307	3.0	45.0	29.6	0.313	981	19.6	0.286	1072	0.356	862	0.357	859
9	317	3.2	44.9	29.9	0.323	981	19.7	0.296	1071	0.373	850	0.365	869
10	353	3.3	39.3	30.1	0.347	1017	18.5	0.322	1096	0.405	872	0.395	895
11	426	3.8	38.1	30.2	0.397	1073	18.2	0.370	1152	0.458	930	0.453	940
12	509	4.6	36.9	31.9	0.466	1093	18.4	0.437	1165	0.534	953	0.527	966
13	583	5.1	32.2	33.0	0.530	1100	17.5	0.499	1167	0.611	955	0.603	966
14	569	4.9	30.0	32.3	0.531	1071	16.7	0.500	1137	0.641	888	0.634	898
15	709	5.4	28.5	30.0	0.599	1184	15.7	0.566	1253	0.659	1076	0.662	1071
16	824	6.3	26.7	31.3	0.682	1208	15.5	0.644	1279	0.747	1102	0.745	1106
17	882	6.3	27.9	28.3	0.698	1264	15.1	0.662	1332	0.779	1132	0.777	1135
18	925	6.6	26.8	29.0	0.722	1281	15.0	0.685	1349	0.794	1166	0.799	1157
19	939	6.6	27.0	28.0	0.731	1285	14.8	0.695	1351	0.814	1154	0.819	1146
20	862	5.7	22.2	28.4	0.708	1218	13.5	0.666	1295	0.777	1110	0.794	1086
Mean	527	4.4	37.3	30.0	0.466	1095	17.8	0.436	1177	0.522	979	0.520	986

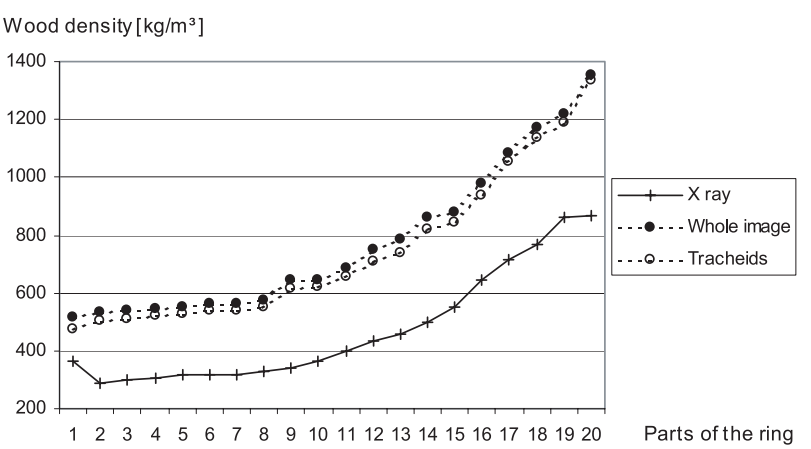

Figure 3. Finland spruce ring: Wood density measured by X-ray and calculated from the cell wall proportion (analysis of the whole image and tracheids only) and a cell wall density of 1530 kg/m³.

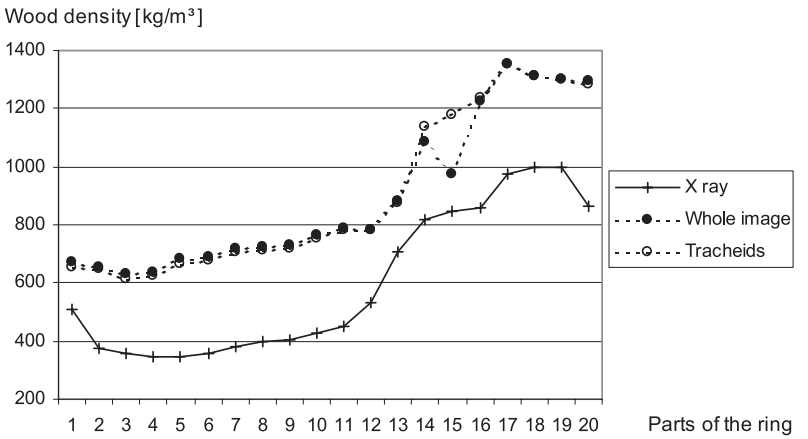

Figure 4. South Finland pine ring: Wood density measured by X-ray and calculated from the cell wall proportion (analysis of the whole image and tracheids only) and a cell wall density of 1530 kg/m³.

Table VII. Planimetric and image analysis measurements on North Finland pine. Length of the window of measurement = ring width = 1280 µm; width of the window of measurement for the planimetry = 1000 µm; width of the window of measurement for image analysis = 1000 µm.

North Finland pine (NFinP)													
		Planimetric measurements								Image analysis			
Parts of the ring	X-ray (kg/m^3)	Cell wall widths (µm)	Radial ϕ (µm)	Tang ϕ (µm)	Cell wall prop. Rect.	Packing density (kg/m^3) Rect.	H (µm)	Cell wall prop. Hexag.	Packing density (kg/m^3) Hexag.	Cell wall prop.	Packing density (kg/m^3)	Cell wall prop. (Masked)	Packing density (kg/m^3) (Masked)
1	433	3.8	35.1	28.1	0.353	1228	16.9	0.328	1319	0.419	1035	0.409	1057
2	371	3.6	35.3	27.4	0.334	1110	16.7	0.310	1196	0.423	876	0.416	893
3	352	3.5	36.9	27.9	0.323	1089	17.2	0.300	1175	0.444	792	0.437	806
4	361	3.4	37.4	28.4	0.328	1102	17.5	0.304	1188	0.446	809	0.438	823
5	362	3.4	37.8	27.2	0.340	1064	17.2	0.314	1153	0.447	809	0.442	818
6	354	3.6	37.2	28.0	0.341	1038	17.3	0.316	1120	0.458	772	0.456	776
7	366	3.8	39.2	28.0	0.347	1053	17.8	0.321	1141	0.458	799	0.456	803
8	376	3.9	42.1	28.0	0.350	1074	18.4	0.321	1172	0.448	840	0.445	844
9	375	4.0	39.7	28.0	0.362	1037	17.9	0.333	1125	0.468	801	0.466	804
10	378	4.1	37.8	28.4	0.362	1045	17.6	0.335	1127	0.470	805	0.468	807
11	396	4.2	39.0	28.4	0.374	1058	17.9	0.346	1144	0.498	795	0.493	804
12	425	4.6	35.1	28.4	0.412	1032	16.9	0.384	1106	0.523	813	0.518	821
13	479	5.6	35.2	28.3	0.443	1082	17.0	0.413	1159	0.549	873	0.542	884
14	530	6.1	33.9	28.3	0.473	1119	16.6	0.443	1196	0.608	872	0.603	879
15	628	6.3	28.5	28.6	0.542	1160	15.4	0.511	1230	0.701	896	0.692	907
16	746	6.1	24.7	27.5	0.655	1139	14.0	0.620	1204	0.708	1053	0.782	953
17	826	6.9	23.1	27.1	0.715	1155	13.4	0.677	1221	0.731	1130	0.859	961
18	921	6.9	23.1	27.5	0.726	1269	13.5	0.686	1342	0.821	1121	0.843	1093
19	959	6.6	22.4	26.6	0.744	1288	13.1	0.705	1360	0.806	1190	0.800	1199
20	875	5.8	19.4	27.0	0.659	1328	12.3	0.613	1427	0.734	1192	0.726	1205
Mean	526	4.8	33.2	27.8	0.459	1124	16.2	0.429	1205	0.558	914	0.565	907

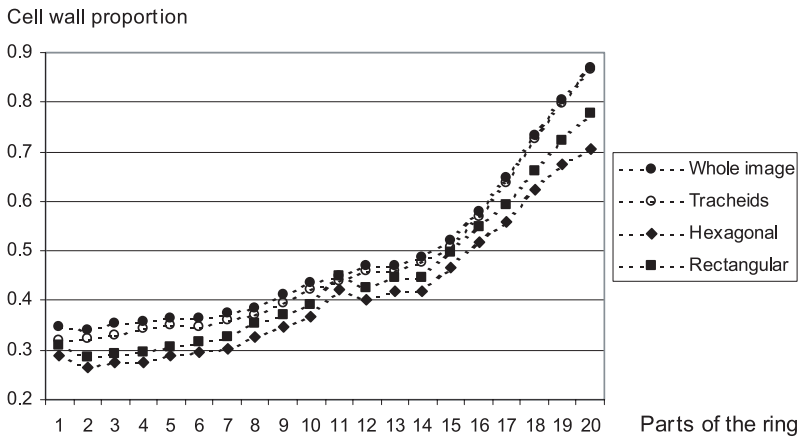

Figure 5. France spruce ring: Cell wall proportion calculated from the rectangular and hexagonal models and measured with image analysis (analysis of the whole image and tracheids only).

Table VIII. Planimetric and image analysis measurements on South Finland pine. Length of the window of measurement = ring width = 2070 µm; width of the window of measurement for the planimetry = 1500 µm; width of the window of measurement for image analysis = 802 µm.

South Finland Pine (SFinP)													
Parts of the ring	X-ray (kg/m^3)	Planimetric measurements								Image analysis			
		Cell wall widths (µm)	Radial ϕ (µm)	Tang ϕ (µm)	Cell wall prop. Rect.	Packing density (kg/m^3) Rect.	H (µm)	Cell wall prop. Hexag.	Packing density (kg/m^3) Hexag.	Cell wall prop.	Packing density (kg/m^3)	Cell wall prop. (Masked)	Packing density (kg/m^3) (Masked)
1	508	3.0	38.8	30.4	0.396	1281	18.4	0.369	1377	0.441	1152	0.426	1193
2	374	2.8	43.3	30.7	0.366	1021	19.6	0.338	1107	0.429	872	0.423	883
3	355	2.8	43.6	31.6	0.350	1016	20.0	0.323	1099	0.413	859	0.402	884
4	346	2.9	39.0	31.2	0.359	964	18.8	0.334	1035	0.418	828	0.408	847
5	348	3.0	38.9	30.9	0.360	968	18.6	0.335	1039	0.445	782	0.435	801
6	360	3.0	41.3	30.6	0.365	986	19.1	0.338	1064	0.451	798	0.442	815
7	383	3.1	39.6	30.0	0.395	968	18.5	0.367	1043	0.469	817	0.462	829
8	398	3.2	38.4	30.2	0.407	979	18.3	0.379	1051	0.473	841	0.465	856
9	406	3.3	39.6	30.1	0.413	983	18.6	0.384	1057	0.478	849	0.468	867
10	427	3.2	36.8	30.6	0.428	998	18.0	0.400	1067	0.499	856	0.491	870
11	453	3.4	35.8	30.3	0.448	1011	17.7	0.419	1080	0.517	877	0.512	884
12	530	3.6	35.8	29.5	0.489	1085	17.5	0.457	1159	0.513	1034	0.512	1036
13	706	4.0	32.8	29.6	0.594	1188	16.7	0.560	1260	0.577	1223	0.573	1232
14	817	4.2	27.8	29.9	0.667	1225	15.5	0.632	1293	0.710	1151	0.742	1101
15	845	4.6	27.0	28.5	0.705	1199	14.9	0.669	1263	0.636	1329	0.771	1096
16	859	5.4	25.2	29.7	0.697	1232	14.7	0.659	1304	0.801	1073	0.810	1060
17	975	5.8	25.2	31.8	0.746	1308	15.2	0.703	1387	0.885	1102	0.884	1102
18	997	6.0	25.9	31.8	0.734	1359	15.4	0.693	1439	0.859	1161	0.858	1162
19	998	6.0	24.0	30.0	0.746	1339	14.4	0.704	1418	0.850	1174	0.849	1175
20	862	4.6	19.8	31.0	0.742	1162	13.3	0.682	1263	0.848	1016	0.840	1026
Mean	597	3.9	33.9	30.4	0.520	1114	17.2	0.487	1190	0.586	990	0.589	986

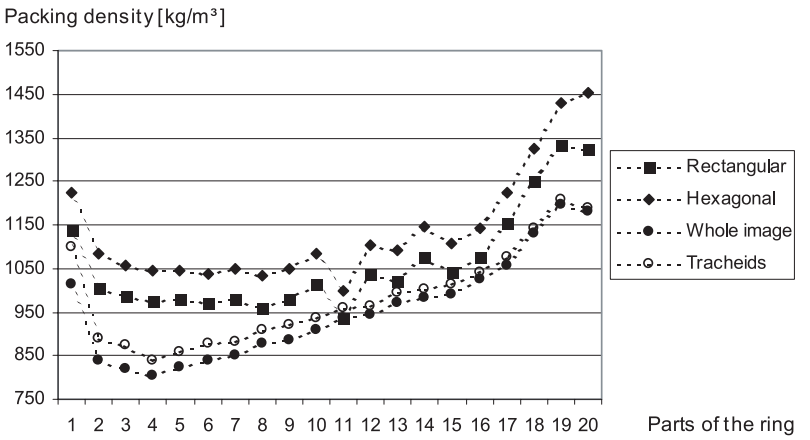

Figure 6. France spruce ring: Packing density (kg/m³) calculated from the rectangular and hexagonal models and measured with image analysis (analysis of the whole image and tracheids only).

3.3. Planimetry compared to image analysis

Fukazawa [13] measured a cell wall proportion in area increasing from ±35% at the beginning to ±90% (80% for the juvenile wood) at the end of the ring and for Quirk [31] it varied from 30 to 90%. Our planimetry and image analysis yield a somewhat lower cell wall proportion, but in the same range of variation.

The cell wall proportion obtained by the different methods (Tabs. III to VIII) rises from, in order, planimetry with the hexagonal model, planimetry with the rectangular model, image analysis on masked image to image analysis on whole ring image. This is illustrated on the Figures 5 and 6. As planimetry uses a cell shape model, the calculated proportion is that of the tracheid walls only and this proportion will thus logically be inferior than those measured with image analysis. When rays and canal walls are excluded the measured proportion gets closer to the planimetric results.

The methods themselves are also responsible for some of those differences. The use of a rectangular or hexagonal model for the tracheid shape leads to simplifications. Those models assume that the cell wall thickness is constant all around the perimeter of the cells. The hexagonal one also supposes the equality of the radial and tangential dimensions of the tracheids.

4. DISCUSSION

4.1. Apparent density of the cell wall

After Stamm's 1929 works, inferior cell wall and wood substance densities were obtained by physical measurements (helium, mercury, benzene and toluene displacements). A mean value of 1460 kg/m³ which may be considered as the dry cell wall density value, and also as the density of the dry wood substance (as the dry cell wall would be essentially non porous [34, 35, 39, 40, 42, 44]) may be brought out for conifers [4, 19, 38, 39, 43–45].

Planimetry and image analysis both give apparent cell wall density values of around 1000–1400 kg/m³, values different from 1530 kg/m³ and 1460 kg/m³.

The literature points out that all the optical estimations of the apparent density of the cell wall [19, 30, 32, 33, 41, 43, 47] show a clear tendency for being far weaker than the value of 1460 kg/m³. Only Quirk [29] obtains values closer to 1460 kg/m³.

To our knowledge there is not only one unique explanation of this difference between the value of 1000 and 1460 kg/m³ but some suppositions can be made.

• The quality of the observed sample is of great importance. The measurements using automated microscopy on wood sections are at least as accurate as any other practical quantification method but there is a requirement that the samples be free from damage, thin and uniformly stained. Danborg [5] working with image analysis mentions that the quality of the image depends on the quality of the microtome section, and the quality and resolution of the microscope and camera. Indeed, intercellular spaces are only detected if the system's resolution allows it.

• Some corrections should be applied in view of the measurements conditions.

– The thickness of the section may be responsible for a parallax problem leading to an overestimation of the cell wall area [1, 5, 25]. A correct focus during the acquisition of the images is thus essential. For Donaldson [6], there can be an effect of "out-of-focus" due to the thickness of the sections and ray cells and pits may be filled by the inclusion of lateral walls on the deepness of the image.

– The treatment of the wood sample leading to the measured support (section) may not leave the wood intact. Fengel [11] reports in this way that fibres are getting thicker during wood impregnation as the polymerisation reaction occurs in a media that penetrates into the fibre quicker than in the outside media. Wood slicing may also be responsible of an increase of the cell wall area [19].

– During drying, sections are subjected to shrinkage and this latest would be responsible of a reduction [6, 7, 30] or of an increase [19] of the cell wall proportion.

– The moisture content of a mounted section is not known with accuracy and according to Boutelje [2] the observed shrinkage varies with the used drying technique.

• Even if rays and canals are excluded, the measured area proportion is that of the visible material on a transverse plane that is the cell wall but also the middle lamellae, the cell wall thickenings in contact of the rays. All the pre-existing but also the eventual neo-formed voids, that aren't detected, are also considered as part of the matter. Those voids may play a great role in the difference between the optically assessed packing density of around 1000 kg/m³ and the cell wall density measured directly on wood substance of around 1460 kg/m³.

4.2. Interpretation of the intra ring wood density variations

From EW to LW, the wood density increase is the consequence of (i) anatomical modifications: increase of the cell wall width and increase of the number of cell rows in both directions (but more slightly in the tangential direction) and (ii) chemical ones: the cell wall density increases slightly from EW to LW as a consequence of the variation of the structure and chemical composition of the cell wall.

The anatomical changes are mainly responsible for the wood density variations as the packing density variations play only a minor role.

4.2.1. Anatomical point of view: cells sizes measured by planimetry

From EW to LW the tracheids become smaller and their walls thicker. These anatomical variations result in an increase of the cell wall proportion all along the ring. The changes of the cells sizes are greater in the radial [9, 17] than in the tangential direction [8] as the number of cells rows increases much more in the radial than in the tangential direction.

The more important variation of the cell wall thickness compared to those of the cells size as already observed [12, 15] confirms that the cell wall thickness variations play a major role in the wood density variations.

4.2.2. Chemical point of view: evolution of the apparent density of the cell wall

The calculated apparent density of the cell wall (with both methods) shows a slight increase from EW to LW that may be explained by anatomical and chemical considerations.

In the LW the cell walls thickness of the S_2 (the richest in cellulose) and S_1 layers, are strongly and weakly thicker than in the EW, respectively while the S_3 layer and the primary wall have almost the same thickness all along the ring [10].

Stamm [37] notices that the compound middle lamella (primary wall and middle lamella together) is much thicker in the LW than in the EW as for Fukazawa [13], the middle lamella proportion in relation to the entire cell wall is of 10–15% and stays practically constant all along the ring. As LW fibres are more circular, more middle lamella is found at the junction of four fibres [37]. The taking into account of the middle lamella in the area measurements would thus play a more important role in the LW.

From a chemical point of view, the composition of the cell wall also varies, explaining a superior cell wall density in LW than in EW. Yiannos [47] finds LW cell wall densities superior by at least 100 kg/m³ than in EW. Wilfong's [45] observations also point in that direction and his explanation is that the thicker S_2 layer and the higher cellulose content of the LW cell wall account for the difference observed. Stamm [37] confirms the increase of the cellulose content of the cell wall from EW to LW and observes an increase of the cell wall density from EW (1416 kg/m³) to LW (1450 kg/m³) for the rings close to the pith, but this increase becomes negligible for rings 26 to 33 on average: cell wall density = 1459 for the EW and 1461 kg/m³ for the LW.

5. CONCLUSIONS

We have verified that the knowledge of the (i) tracheid geometry and (ii) the usually admitted value of the cell wall density allow us to calculate intra ring wood density profiles which are similar in terms of variations than the X-rays wood density profiles but very different in average. Thus it appears at least necessary to calibrate carefully the optical measurement by using an apparent cell wall density which is far weaker from the effective cell wall density of 1460 kg/m³ obtained by physical measurements. In addition this calibration needs to vary inside the ring in order to match perfectly both profiles according to the method used for the determination of the cell wall proportion (Fig. 6). The effects of the treatments of the wood sample (embedding, slicing, drying…) and of the image of the rings (acquisition procedure, thresholding…) should be carefully tested and accurately quantified.

Based on this result gained for raw material from three important softwood species, a further and useful development could be to test how and if it is possible to determine, for a given and known species, the tracheid geometry variations directly from the intra ring density profile.

Acknowledgements: We would like to thank Simone Garros who prepared all the sections of this study. Funding for this work was provided by a Belgian F.N.R.S. PhD research grant to Valérie Decoux and by a French grant from the "Région Lorraine".

REFERENCES

[1] Berlyn G.P., A Hypothesis for Cell Wall Density, For. Prod. J. 18 (1968) 34–36.

[2] Boutelje J., On shrinkage and change in microscopic void volume during drying, as calculated from measurements on microtome cross sections of Swedish Pine (*Pinus sylvestris* L.), Svensk Papperstidning 65 (1962) 209–215.

[3] Brown H.P., Panshin A.J., Forsaith C.C., Textbook of wood technology, Vol. 1, McGraw-Hill Book Co., Inc., New York, NY, 1949.

[4] Christensen G.N., Hergt H.F.A., The Apparent Density of Wood in Non-Swelling Liquids, Holzforschung 22 (1968) 165–170.

[5] Danborg F., Pedini M., The use of X-ray densitometry and digital image analysing for wood technological research, Internal of the

Royal Veterinary and Agricultural University, Department of Economics and Natural Resources, KVL, Hrsholm, Denmark, 1990.

[6] Donaldson L.A., Lausberg M.J.F., Comparison of conventional transmitted light and confocal microscopy for measuring wood cell dimensions by image analysis, IAWA J. 19 (1998) 321–336.

[7] Ellwood E.L., Wilcox W.W., The Shrinkage of Cell Walls and Cell Cavities in Wood Microsections, For. Prod. J. 12 (1962) 235–242.

[8] Erickson H.D., Harrison A.T., Douglas - Fir Wood Quality Studies, Part I: Effects of Age and Stimulated Growth on Wood Density and Anatomy, Wood Sci. Technol. 8 (1974) 207–226.

[9] Fengel D., Stoll M., On the Variation of the Cell Cross Area, the Thickness of the Cell Wall and of the Wall Layers of Sprucewood Tracheids within an Annual Ring, Holzforschung 27 (1973) 1–7.

[10] Fengel D., The Ultrastructure of Cellulose from Wood, Part I: Wood as the Basic Material for the Isolation of Cellulose, Wood Sci. Technol. 3 (1969) 203–217.

[11] Fengel D., Ultramicrotomy, Its Application in Wood Research, Wood Sci. Technol. 1 (1967) 191–204.

[12] Ferrand J.C., Réflexions sur la densité du bois, 1e Partie: Définition de la densité du Bois, Holzforschung 36 (1982) 99–105.

[13] Fukazawa K., Imagawa H., Quantitative Analysis of Lignin Using an UV Microscopic Image Analyser. Variation Within One Growth Increment, Wood Sci. Technol. 15 (1981) 45–55.

[14] Hannrup B., Danell O., Ekberg I., Moëll M., Relationships between wood density and tracheid dimensions in *Pinus sylvestris* L., Wood Fiber Sci. 33 (2001) 173–181.

[15] Heger L., Parker M.L., Kennedy R.W., X-Ray Densitometry: A Technique and An Example of Application, Wood Sci. 7 (1974) 140–148.

[16] Ifju G., Within-Growth-Ring Variation in Some Physical Properties of Southern Pine Wood, Wood Sci. 2 (1969) 11–19.

[17] Ivkovich M., Koshy M.P., Wood Density Measurement: Comparison of X-ray, Photometric, and Morphometric Methods, Timber Management Toward Wood Quality and End-Product Value, CTIA/IUFRO International Wood Quality Workshop, 1997.

[18] Jayme G., Krause T., Uber die Packungsdichte der Zellwände in Laubhölzern, Holz Roh- Werkst. 21 (1963) 14–19.

[19] Kellogg R.M., Wangaard F.F., Variation in the cell-wall density of wood, Wood Fiber 1 (1969) 180–204.

[20] Koubaa A., Zhang S.Y.T., Makni S., Defining the transition from earlywood to latewood in black spruce based on intra-ring wood density profiles from X-ray densitometry, Ann. For. Sci. 59 (2002) 519–524.

[21] Lindström H., Fiber length, tracheid diameter, and latewood percentage in Norway spruce: Development from pith outwards, Wood Fiber Sci. 29 (1997) 21–34.

[22] Mörling T., Evaluation of annual ring width and ring density development following fertilisation and thinning of Scots pine, Ann. For. Sci. 59 (2002) 29–40.

[23] Mothe F., Duchanois G., Leban J.M., Owoundi R.E., Perrin J.R., Qualification des bois par microdensitométrie, Contrat Région Lorraine – INRA, Décision DBCR 158–90 (Code INRA 3086A), 1990.

[24] Mothe F., Duchanois G., Zannier B., Leban J.-M., Analyse microdensitométrique appliquée au bois: méthode de traitement des données utilisée à l'Inra-ERQB (programme Cerd), Ann. Sci. For. 55 (1998) 301–313.

[25] Park W-K., Telewski F.W., Measuring maximum latewood density by image analysis at the cellular level, Wood Fiber Sci. 25 (1993) 326–332.

[26] Polge H., Fifteen Years of Wood Radiation Densitometry, Wood Sci. Technol. 12 (1978) 187–196.

[27] Polge H., Établissement des courbes de variation de la densité du bois par exploration densitométrique de radiographies d'échantillons prélevés à la tarière sur des arbres vivants – Applications dans les domaines technologique et physiologique, Ann. Sci. For. 23 (1966) 1–215.

[28] Polge H., Le bois juvénile des conifères, Rev. For. Fr. 86 (1964) 473–505.

[29] Quirk J.T., Cell Wall Density of Douglas Fir by two Optometric Methods, Wood Fiber Sci. 16 (1984) 224–236.

[30] Quirk J.T., Shrinkage and related properties of Douglas-fir cell walls, Wood Fiber Sci. 16 (1984) 115–133.

[31] Quirk J.T., Dot-grid integrating eyepiece: two sampling techniques for estimating cell wall areas, Wood Sci. 8 (1975) 88–91.

[32] Quirk J.T., Smith D., Comparison of dual linear and dot-grid eyepiece methods for estimating wood properties of Douglas-fir, Wood Sci. 8 (1975) 92–96.

[33] Smith D.M., Rapid Measurement of Tracheid Cross-Sectional Dimensions of Conifers: Its Application to Specific Gravity Determinations, For. Prod. J. 15 (1965) 325–334.

[34] Stamm A.J., History of Two Phases of Wood Physics, Wood Sci. Technol. 1 (1967) 186–190.

[35] Stamm A.J., Wood and Cellulose Science, North Carolina State of the University of North Carolina at Raleigh, 1964.

[36] Stamm A.J., Density of wood substance, absorption by wood, and permeability of wood, J. Phys. Chem. 33 (1929) 398–414.

[37] Stamm A.J., Sanders H.T., Specific Gravity of the Wood Substance of Loblolly Pine as Affected by Chemical Composition, Tappi 49 (1966) 397–400.

[38] Stayton C.L., Hart C.A., Determining Pore-Size Distribution in Softwoods with a Mercury Porosimeter, For. Prod. J. 15 (1965) 435–440.

[39] Stone J.E., Scallan A.M., Aberson G.M.A., The Wall Density of Native Cellulose Fibres, Pulp and Paper Research Institute of Canada 67 (1966) T263–T268.

[40] Stone J.E., Scallan A.M., A Study of Cell Wall Structure by Nitrogen Adsorption, Pulp and Paper Research Institute of Canada 66 (1965) T407–T414.

[41] Tsoumis G., Microscopic Measurement of the Amount of Cell Wall Substance in Wood and Its Relationship to Specific Gravity, Tappi 47 (1964) 675–677.

[42] Tsoumis G., Passialis C., Effect of growth rate and abnormal growth on wood substance and cell-wall density, Wood Sci. Technol.11 (1977) 33–38.

[43] Wangaard F.F., Cell-Wall Density of Wood With Particular Reference to the Southern Pines, Wood Sci. 1 (1969) 222–226.

[44] Weatherwax R.C., Tarkow H., Cell Wall Density of Dry Wood, For. Prod. J. 18 (1968) 83–85.

[45] Wilfong J.G., Specific Gravity of Wood Substance, For. Prod. J. 16 (1966) 55–61.

[46] Wimmer, R., Intra-annual cellular characteristics and their implications for modeling softwood density. Wood Fiber Sci. 27 (1995) 413–420.

[47] Yiannos P.N., The apparent Cell-Wall Density of Wood and Pulp Fibers, Tappi 47 (1964) 468–471.